Journal of the Meteorological Society of Japan, Vol. 87, No. 4, pp. 665–685, 2009.
DOI:10.2151/jmsj.87.665

Air Mass Transformation along Trajectories of Airflow and Its Relation to Vertical Structures of the Maritime Atmosphere and Clouds in Yamase Events

Yasu-Masa KODAMA

Department of Earth and Environmental Sciences, Graduate School of Science and Technology, Hirosaki University, Hirosaki, Japan

Yoshiaki TOMIYA and Shoji ASANO

Center for Atmospheric and Oceanic Studies, Tohoku University, Sendai, Japan

(Manuscript received 27 October 2008, in final form 8 April 2009)

Abstract

The Yamase is a cool easterly wind that is observed in summer along the eastern coast of the northern part of the main island (Honshu) of Japan. It usually accompanies a boundary layer cloud, the "Yamase cloud." The origin of the Yamase is the cool polar maritime air mass that develops over the North Pacific, including the Bering Sea and the Sea of Okhotsk. The characteristics of the Yamase are controlled by air mass transformation over the western North Pacific. Campaign observations of the Yamase were performed using the marine vessel Koufu-maru of the Japan Meteorological Agency over the sea east of northern Honshu in summer, from 2001 to 2007. We studied two Yamase events and examined the heat flux along back trajectories as well as the heat and moisture budget. The vertical structure of the Yamase was strongly dependent on the history of the air over the ocean, despite the many factors that influence boundary layer clouds. In the June 2003 event, the stepwise upward development of Yamase clouds observed at the Koufu-maru site was related to the influence of Hokkaido Island and an oceanic front on Yamase flow trajectories. For the July 2006 event, the temperature profiles observed from the Koufu-maru changed from stable layer type to mixed layer type. Changes in the visibility and oceanic heating along Yamase air trajectories were also observed. Ocean heating increased when the trajectories changed from westward to southward across an oceanic front located to the east of 144°E in the Kuroshio-Oyashio extension. The meridional SST gradient was smaller over water off northern Honshu, where the Oyashio current prevailed. A heat and moisture budget analysis using aerological data observed by the Koufu-maru and three weather stations in northern Japan showed weak sensible heating and weak moisture sink when the Yamase wind prevailed. We ascribed the weak sensible heating to the small air–sea temperature difference, which was caused by the weak meridional SST gradient and offset by radiative cooling at the cloud top.

1. Introduction

The "Yamase" is a cool easterly wind observed in summer along the eastern coast of the Sanriku district, on the Pacific side of the northern part of Honshu Island, Japan (Fig. 1). The origin of the Yamase is the cool polar maritime air mass that develops over the North Pacific, including the Bering Sea and the Sea of Okhotsk. The air mass is transported by 1000-km-scale low-level flow in the atmospheric boundary layer (referred to here as "Yamase flow"), which develops over the western North Pacific and forms along the southern and southeastern peripheries of the Okhotsk High. Due to the abundant moisture supply from the ocean, the Yamase is wet and is usually accompanied by

Corresponding author: Yasu-Masa Kodama, Department of Earth and Environmental Sciences, Graduate School of Science and Technology, Hirosaki University, Hirosaki, Aomori, 036-8561 Japan.
E-mail: kodama@cc.hirosaki-u.ac.jp

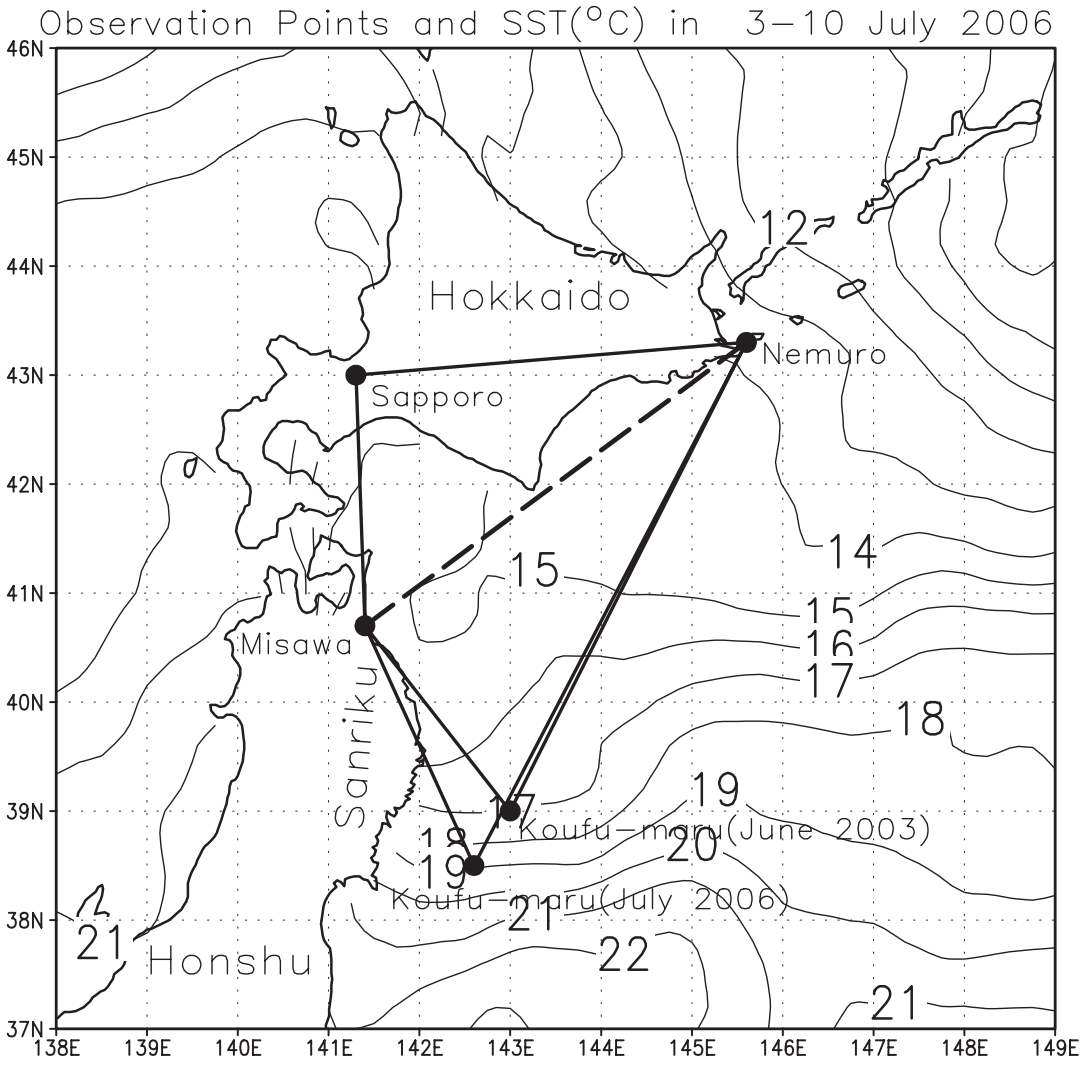

Fig. 1. SST field averaged between 3 and 10 July 2006. Positions of the aerological stations, along with approximate positions of the Koufu-maru during the intensive observation periods in June 2003 and July 2006, are shown. In the budget analysis by Ninomiya and Mizuno (1985), three stations were used: Nemuro, Sapporo, and Misawa. In the present study, four stations were used: the three listed above and the Koufu-maru.

maritime boundary layer (MBL) clouds, which are called "Yamase clouds" (Urano et al. 1990; Kojima et al. 2006). The Okhotsk High sometimes stagnates around the Okhotsk Sea because of blocking phenomena. At this time, a long-lasting (several days to 1 month) Yamase occurs and damages rice crops in the Sanriku district due to the lower temperatures and reduced sunshine caused by clouds.

As discussed by Nagasawa et al. (2006), MBL clouds are maintained by many processes, such as heat and moisture supply from oceans, vertical mixing of heat and moisture in the MBL, and radiative and evaporative cooling at the top of the clouds. Yamase clouds develop over the western North Pacific, where there is a large meridional sea surface temperature (SST) gradient between the Kuroshio warm and Oyashio cold currents. Figure 1 shows the SST field from July 3 to 10, 2006, which was one of our study periods. Note the strong meridional SST gradient along 40.5°N to the east of 144°E, which is a subarctic (Oyashio)

oceanic front (Yuan and Talley 1996; Nonaka et al. 2006). The SST gradient was weaker to the west of 144°E off the Sanriku coast to the north of 39°N due to intrusion of the Oyashio cold current. An oceanic front was located around 38°–39°N at this longitude. Similar features were also observed from June 20 to 24, 2003, which was another period chosen for this study. The oceanic fronts may cause air mass transformation of the Yamase and influence clouds when the Yamase flows across the contours of SST. In situ observations of the Yamase over the sea are important for describing the formation process of Yamase clouds. However, few such observations have been reported to date (Gorai and Sasaki 1990), and many of the studies reviewed below were based on land observations in northern Japan or on satellite remote sensing.

Ninomiya and Mizuno (1985) analyzed heat budgets for two Yamase cases observed in the summers of 1976 and 1980, using operational aerological observations from three stations over northern Japan (Sapporo, Misawa, and Nemuro; Fig. 1). They found that the mixed layer in the Yamase was shallow (~1 km). Although total heating of the lower atmosphere was ~5 K/day, the total heat supply from the sea, estimated from vertical integration of the Yamase flow, was 45 to 65 W/m^2. This weak heating was ascribed to the small air–sea temperature difference (~2°C) over the study region. The study region of Ninomiya and Mizuno (1985) was a narrow stretch of water between Hokkaido and Honshu surrounded by three stations (Fig. 1) and did not overlap the region of large total heat flux to the east of ~144°E (Kodama 1997).

In the summer of 1993, the Yamase continued for about 1 month and damaged rice crops in the Sanriku district. Kodama (1997) examined synoptic-scale variations of boundary layer and Yamase clouds observed along the Sanriku coast and noted marked variation in the vertical structure of the Yamase and its clouds. Vertical profiles of temperature and moisture observed at Misawa (40.7°N, 141.4°E), in the northern part of the Sanriku district (Fig. 1), were classified into two types. The first was the ''mixed layer type,'' which was accompanied by an atmospheric mixed layer topped by Yamase clouds. The cloud base was not usually attached to the sea surface in this type. The second was the ''stable layer type,'' which was accompanied by a stable layer attached to the surface, where Yamase clouds also formed. The bottom of the cloud layer was usually attached to the sea surface for this type, forming sea fog. The back trajectories of the Yamase flow over the North Pacific differed between the two types. Mixed layer type Yamase flow over the North Pacific was southwestward, coming directly from the Bering and Okhotsk Seas toward the Sanriku coast. Cold air flew over a relatively warmer ocean, and an atmospheric mixed layer formed. Along the Sanriku coast, the observed air temperature of the Yamase was lower than that of the SST. Stable layer type Yamase flow was southwestward over the western Pacific, turning northwestward off the Sanriku coast. The flow was warm-advective off the Sanriku coast, and a stable layer with advection fog may develop. Kodama (1997) found that the heat flux changed according to the direction of the Yamase flow because of the large meridional gradient of the SST. The total (sensible and latent) heat flux was positive when the flow was southward, and weakly positive or negative when it was northward. Using a bulk method, Kodama (1997) showed that total heat flux over the ocean occasionally reached 100 W/m^2 to the east of 144°E when the Yamase flow was strong and southwestward. Moreover, he also found a unique case when the Yamase was cold and dry on the Sanriku coast. The back trajectory of the Yamase was from Hokkaido (Fig. 1), and the flow was not moistened, due to the short distance over the water between the Hokkaido and Sanriku coasts. Kodama (1997) used profiles of Yamase air observed at Misawa, which may have been influenced by land surface processes. In situ observations of Yamase air profiles over the ocean were expected for future study.

Takai et al. (2006) examined large-scale wind fields over the western North Pacific using sea wind observations with a satellite scatterometer. They also examined the relation of the Yamase to the surface air temperature variation over northern Honshu north of 36°N. They noted that all of northern Honshu showed a significant negative temperature anomaly when the Yamase blew southwestward directly along the Kuril Islands. In contrast, only the Pacific side was affected when the Yamase blew southwestward from the sea south of the Kuril Islands.

To describe the Yamase and the associated air–sea interaction over the ocean, campaign observations were performed by a collaboration that included the Center for Atmospheric and Oceanic Studies (CAOS) of Tohoku University, the Sendai

District Meteorological Observatory, and the Hakodate Marine Observatory (HMO) of the Japan Meteorological Agency (JMA) in the early summer of 2001 through 2007. The marine observation vessel Koufu-maru of HMO observed the eastern waters of the Sanriku coast (Kojima et al. 2006). As significant Yamase events occur only every few years, long observation periods are necessary. During this period, two Yamase events were observed in late June 2003 and early July 2006. The vertical structure of the maritime atmosphere during Yamase events was described using aerological observation data. The data were obtained by GPS sondes launched from the Koufu-maru, which was located near an oceanic front at the southern end of the Oyashio intrusion (Fig. 1). Many other useful observations, including SST, surface wind, temperature, relative humidity, visibility, and cloud base height were made at this site.

From the vessel observation in June 2003, Kojima et al. (2006) found significant stepwise development of Yamase clouds during the period between June 22 and 25 using aerological observations from the Koufu-maru at approximately 39°N, 143°E off the Sanriku coast (Fig. 1). In this case, the optical and physical features of the Yamase clouds were examined using data from the Advanced Very High Resolution Radiometer (AVHRR) on NOAA-17 and the microwave radiometer onboard the vessel. The drop size of the Yamase clouds increased with their upward development.

In the present study, we examined the relationships between the vertical structure of MBL, the sea–air temperature difference, and visibility observed by the Koufu-maru vessel for the two cases in late June 2003 and July 2006. Such observations were free from the direct influence of the land surface. We also investigated the transformation of Yamase airflow over the ocean along the back trajectories to the Koufu-maru positions in relation to the observed Yamase at the vessel. SST data with high horizontal resolution were utilized to examine the influence of oceanic fronts.

For the late June 2003 case, the early stage of a remarkably long-lasting Yamase continuing for about 1 month was observed. We examined the mechanisms of the stepwise development of Yamase clouds found by Kojima et al. (2006) by considering changes in atmospheric heating along the back trajectories of the Yamase flow in relation to airflow over the ocean and the influence of oceanic fronts. In the early July 2006 case, a weak Yamase was observed for most of the whole period. In July 2006, the Koufu-maru observed another Yamase event when an Okhotsk anticyclone stagnated for about 1 week. In this case, two typical profiles of Yamase MBL similar to those proposed by Kodama (1997) were observed from the vessel. We examined the relationship between alternations of the profiles and changes in heating along the back trajectories of the Yamase airflow. We also performed heat and moisture budget analyses using aerological observation data from the Koufu-maru, along with other routine observations from the land sites. The study region of Ninomiya and Mizuno (1985) was thus extended southward (Fig. 1).

2. Data analysis procedure

We investigated the vertical structure of Yamase air using 3–12-hourly GPS sonde observations launched from the Koufu-maru. The vessel remained at approximately 39°N, 143°E in June 2003 and 38.5°N, 142.5°E in July 2006 (Fig. 1). We also used visibility and cloud base height data, as well as routine aerological observations from the Nemuro (43.3°N, 145.6°E), Sapporo (43.0°N, 141.3°E), and Misawa (40.7°N, 141.4°E) stations (Fig. 1) to describe the spatial variation of the MBL and to perform heat and moisture budget analyses.

The heat and moisture budget analyses were performed using aerological observations at these four points. The heat and moisture budgets are described using $Q1$ (apparent heat source) and $Q2$ (apparent moisture sink), as described previously (Yanai et al. 1973; Yanai and Johnson 1993; Yanai et al. 1992). Here, $Q1$ and $Q2$ are defined as follows:

$$Q1 = Cp(p/p0)^{R/Cp}(\partial\bar{\theta}/\partial t + \bar{\vec{v}}\cdot\nabla\theta + \bar{\omega}\partial\bar{\theta}/\partial p), \quad (1)$$

$$Q2 = -L(\partial\bar{q}/\partial t + \bar{\vec{v}}\cdot\nabla\bar{q} + \bar{\omega}\partial\bar{q}/\partial p). \quad (2)$$

In (1) and (2), $\bar{}$ denotes the area average, θ is the potential temperature, ω is the vertical p-velocity Omega, q is the mixing ratio, $\vec{v}$ is the horizontal velocity, Cp is the specific heat of dry air, and L is the latent heat of condensation. $Q1$ and $Q2$ are residuals of the heat and moisture budgets of the resolvable motion and may be interpreted as

$$Q1 = Q_R + L(\bar{c} - \bar{e}) - \frac{\partial}{\partial p}\overline{s'\omega'}, \quad (3)$$

$$Q2 = L(\bar{c} - \bar{e}) + L\frac{\partial}{\partial p}\partial\overline{q'\omega'}, \quad (4)$$

where $s \equiv C_p T + gz$ is the dry static energy, and L, c, e, and Q_R are the latent heat, condensation rate, evaporation rate, and radiative heating rate, respectively. $Q1$ includes latent heating, radiative heating, and apparent heating by convergence of the turbulent vertical heat flux. $Q2$ includes latent heating and moisture sink by divergence of the turbulent vertical moisture flux. Ninomiya and Mizuno (1985) defined total heating as $\frac{d}{dt}\left(T + \frac{Lq}{Cp}\right)$, which is approximated by $(Q1 - Q2)/Cp$ in the atmospheric boundary layer where T (air temperature) is close to the potential temperature. We calculated Omega, which was also used to evaluate $Q1$ and $Q2$, by vertical integration of the divergence of horizontal wind, using the continuity equation and horizontal wind observed at four stations (Sapporo, Nemuro, Misawa, and the Koufu-maru; Fig. 1). Omega was corrected to be zero at 300 hPa using the method of O'Brien (1970). The reliability of the budget analysis was strongly dependent on Omega, which could not be observed directly, and was evaluated from horizontal wind using the mass continuity equation. To examine the quality of our estimate, we calculated Omega using different combinations of three observation points from among the four points. The time sequences of the Omega profiles were not markedly different (data not shown).

To examine the air mass transformation over the ocean, we analyzed the back trajectories of Yamase air observed on the Koufu-maru using a system in the "METeolorogical Data Explorer" (METEX[1]) developed by the National Institute of Environmental Studies/Center for Global Environmental Research (NIES/CGER; Zeng et al. 2003). This system calculates 3D trajectories kinematically using temporally and spatially interpolated wind vectors derived from 6-hourly NCEP/NCAR reanalysis data with horizontal resolution of $2.5^\circ \times 2.5^\circ$. We examined 3-day back trajectories of Yamase air from the vessel point at a mean sea level (MSL) of 120 or 160 m every 6 h during the study periods. The 120 or 160 m MSL was higher than the observation height on the Koufu-maru but was selected as the minimum height to prevent touchdown of the back trajectories, which terminated the calculation in the METEX system. This problem was caused by the neglect of vertical mixing due to subgrid-scale wind variation in the MBL in the calculation. Because 120 or 160 m MSL at the site was located within the Yamase cool layer at the Koufu-maru site even when the cool layer was shallow, the back trajectories could approximate the history of Yamase air in the MBL. The results can be regarded as references to the surface air observations at the Koufu-maru, which were also within the Yamase cool layer. We confirmed that back trajectories were not as sensitive to the height at the vessel points, because the results from the vessel point at 200 m MSL were not largely different from those at 120 or 160 m MSL, especially in the last 2 days in the back trajectories (data not shown). Omega values in the NCEP/NCAR data were different from those derived from aerological data, which were utilized in heat and moisture budget analyses (data not shown). This seems reasonable because the NCEP/NCAR reanalysis does not have sufficient resolution to describe meso-scale vertical wind for the area of our budget study. No correction was applied for Omega of NCEP/NCAR reanalysis for back trajectory analysis, because vertical displacement of back trajectories was not large in our cases.

We also used cloud images observed by a geostationary satellite (GOES-9) obtained from the archives of Kouchi University, and New Generation Sea Surface Temperature (NGSST) data (Guan and Kawamura 2004), which have high spatial ($0.05^\circ \times 0.05^\circ$) and temporal (daily) resolution and hence can describe the behavior of oceanic fronts. The NGSST data provided objectively merged SST fields derived from several satellite observations; infrared radiometry from the MODerate resolution Imaging Spectroradiometer (MODIS) and the AVHRR; and microwave radiometry from the Advanced Microwave Scanning Radiometer for EOS (AMSR-E). We also used hourly Grid Point Value (GPV) data from a JMA numerical prediction by a regional spectral model of $0.2^\circ \times 0.25^\circ$ (latitude/longitude) resolution, along with the NGSST data, to evaluate the heat flux over the ocean using the bulk method of Kondo (1975). Unfortunately, these data showed weak positive biases in SST and surface air temperature at the Koufu-maru site during the study period. For example, the SST and air temperature at 0 UTC on June 23 observed at the Koufu-maru site were approximately 14.9°C and 13.7°C, respectively. In contrast, the SST obtained from time-interpolated daily GISST data and surface air temperature obtained from GPV data were 15.7°C and 15.4°C at the same point. However, we

1 http://cgermetex.nies.go.jp/metex/trajectory.html

described the total heat flux using these data, because other high-resolution data were not available.

3. June 2003 event

Figure 2 is derived from Fig. 1 of Kojima et al. (2006) and shows time-sequential profiles of air temperature, relative humidity, and wind observed by GPS-sondes launched from the Koufu-maru around 39°N and 143°E, along with cloud base heights measured by a shipboard ceilometer. As emphasized by Kojima et al. (2006), Yamase clouds, along with low-level cool air, developed in a stepwise manner between 22 and 25 June 2003. Hereafter, we refer to a moist layer with relative humidity exceeding 90% as a cloud layer, under a measurement accuracy of $\pm$5% of the GPS-sondes.

The time sequence of the profiles shown in Fig. 2 was as follows. After 0 UTC, June 22, air temperature in the lower troposphere below 300 m MSL began to decrease. After 12 UTC, June 22, a low-level easterly (the Yamase) began, and a shallow cloud layer with top around 300 m MSL was maintained until 0 UTC, June 23. The cloud base was a few tens of meters high (Kojima et al. 2006) and was almost attached to the sea surface. After 0 UTC, June 23, the cloud base detached from the surface and remained around 200 m MSL between 6 and 22 UTC, June 23. The cloud top height increased gradually, reaching 1100 m on 6 UTC, June 24. During this period, the cloud base was raised rapidly to 1000 m between 0 UTC and 3 UTC, June 24. After 6 UTC, June 24, the cloud top and cloud base remained almost constant until 0 UTC, June 25.

Figure 3 shows the time sequence of SST and surface air temperature observed at the Koufu-maru site. Before 10 UTC, June 22, the air temperature exceeded the SST. Between 10 UTC on June 22 and 0 UTC on June 24, the air temperature was lower than the SST. After 0 UTC on June 24, air temperature exceeded the SST again. The air temperature showed diurnal variation, with a minimum around 0 UTC (9 LT) and rapid increase after 0 UTC. This change may have contributed to the diurnal variation observed in the cloud base height, which increased upward after 0 UTC and was lowered during the night between 12 and 21 UTC (Fig. 2), as noted previously (Kojima et al. 2006).

To clarify the mechanisms of the stepwise cloud base height change and surface air temperature variation, we examined 3-day back trajectories of Yamase air from the vessel point at 120 m MSL every 6 h between 18 UTC, June 21, and 12 UTC, June 24 (Fig. 4). The sea level pressure (SLP), averaged over each 3-day period, is also shown. The 120 m MSL at the site was located within the Yamase cool layer observed at the Koufu-maru site throughout the period between June 22 and 24 (Fig. 2a).

Before 18 UTC, June 21, the low-level air came from the Japan Sea, crossing over Honshu, indicating that the observed airflow was not the Yamase (Fig. 4a). At 0 UTC, June 22, the back trajectory changed direction and came from the north, crossing over Hokkaido. The boundary layer air temperature began to decrease at this time (Fig. 2a). Yamase cloud appeared around 10 UTC, June 22, and the air temperature decreased further (Fig. 2). Before the appearance of Yamase clouds, the surface air temperature was higher than the SST at the Koufu-maru site, but it was lower after the appearance of Yamase clouds (Fig. 3).

Figure 5a shows the air temperature profiles over the Koufu-maru at 0 UTC, June 22 and at Sapporo at 0 UTC, June 21, assuming an approximately 1-day difference between these stations along the back trajectory (Fig. 4b). The surface air temperature at Sapporo (17.0°C) was higher than that at the Koufu-maru site (14.7°C). We expected the low-level air from Hokkaido to be cooled over the sea between Hokkaido and the Koufu-maru site; the cooling may have caused a shallow stable layer below 980 hPa at the Koufu-maru site (Fig. 5a). Cooling by the ocean occurred because the SST ($\sim$13.5°C) was lower than the air temperature at the site. By 12 UTC, June 22, after the Yamase cloud covered the sea off the Sanriku coast, the surface air temperature at the site had decreased to around $\sim$14°C, below the SST. We observed a shallow mixed layer with a diabatic temperature lapse rate (Fig. 5b). Radiative and evaporative cooling at the top of the Yamase cloud may have contributed to the decrease in air temperature and helped to maintain the mixed layer. However, the fetch of Yamase flow over the water east off the Sanriku coast was too short between 0 UTC, June 22, and 0 UTC, June 23, to develop a deep mixed layer (Figs. 4b–f). This may also explain why the Yamase cloud was very shallow (Fig. 5b), characterized by small-size cloud droplets during the first stage of the Yamase event (Kojima et al. 2006).

As shown in Fig. 2a, the cloud layer developed upward after 6 UTC, June 23, and the cloud base was detached from the surface. The depth of the

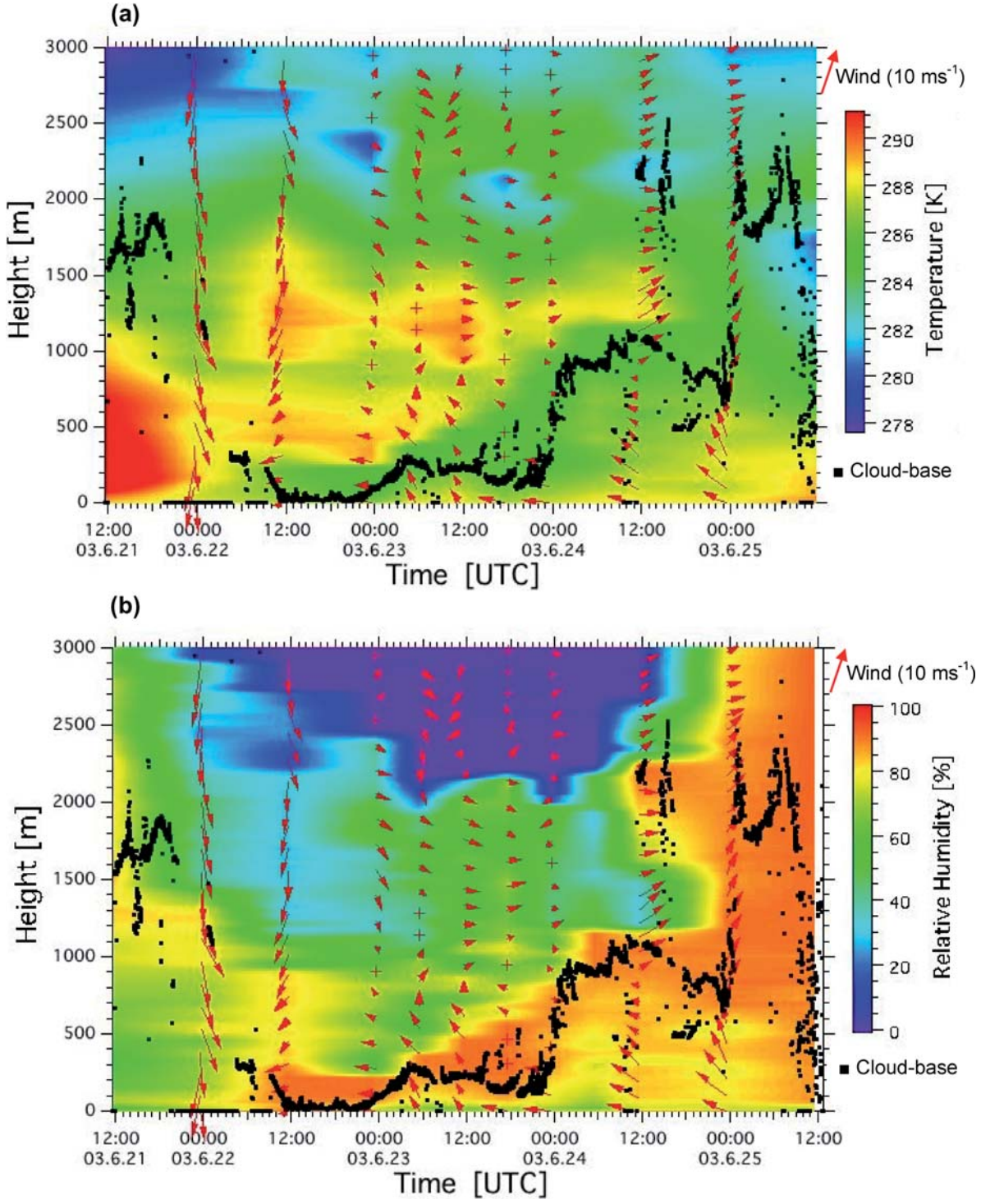

Fig. 2. Time series of air temperature (a) and relative humidity (b) observed at the Koufu-maru site between 12 UTC, June 21, and 12 UTC, June 25, in 2003 (after Kojima et al. 2006).

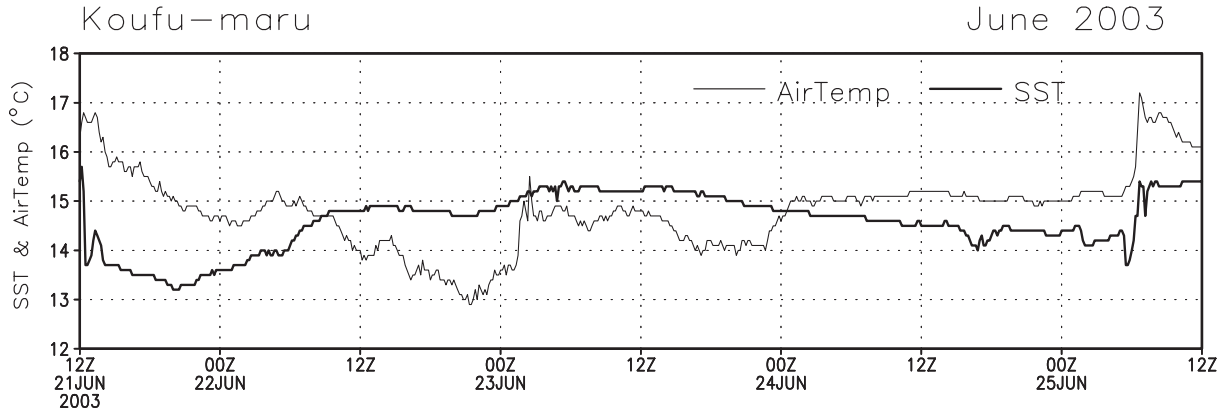

Fig. 3. Time sequence of SST (thick line) and surface air temperature (thin line) observed at the Koufu-maru site between 12 UTC, June 21, and 12 UTC, June 25, in 2003.

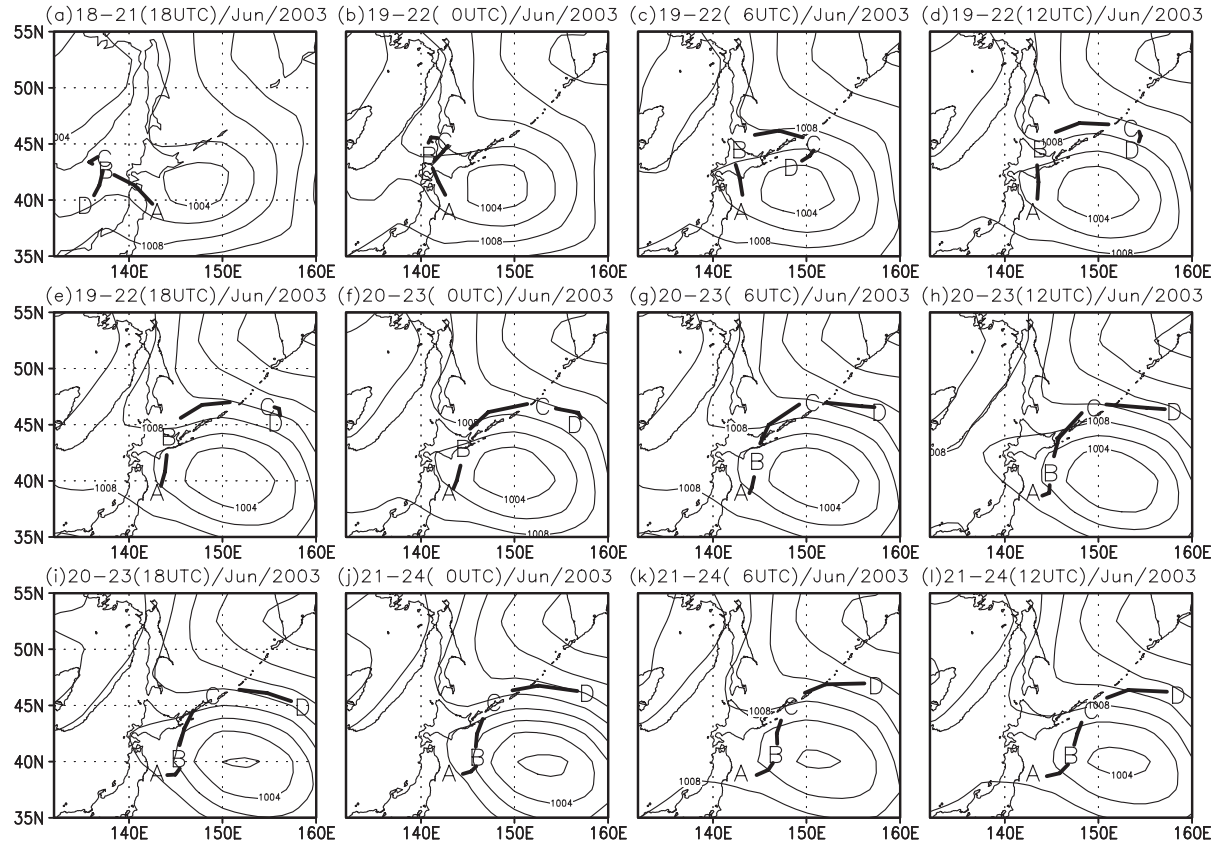

Fig. 4. Three-day back trajectories of low-level air at 120 m MSL above the Koufu-maru site (around 39°N and 143°E). Data were taken every 6 h between 18 UTC, June 21, and 12 UTC, June 24, in 2003. Each panel also shows the SLP averaged over each 72-h period. A, B, C, and D in each panel indicate the air positions at the same time and at 1, 2, and 3 days before, respectively.

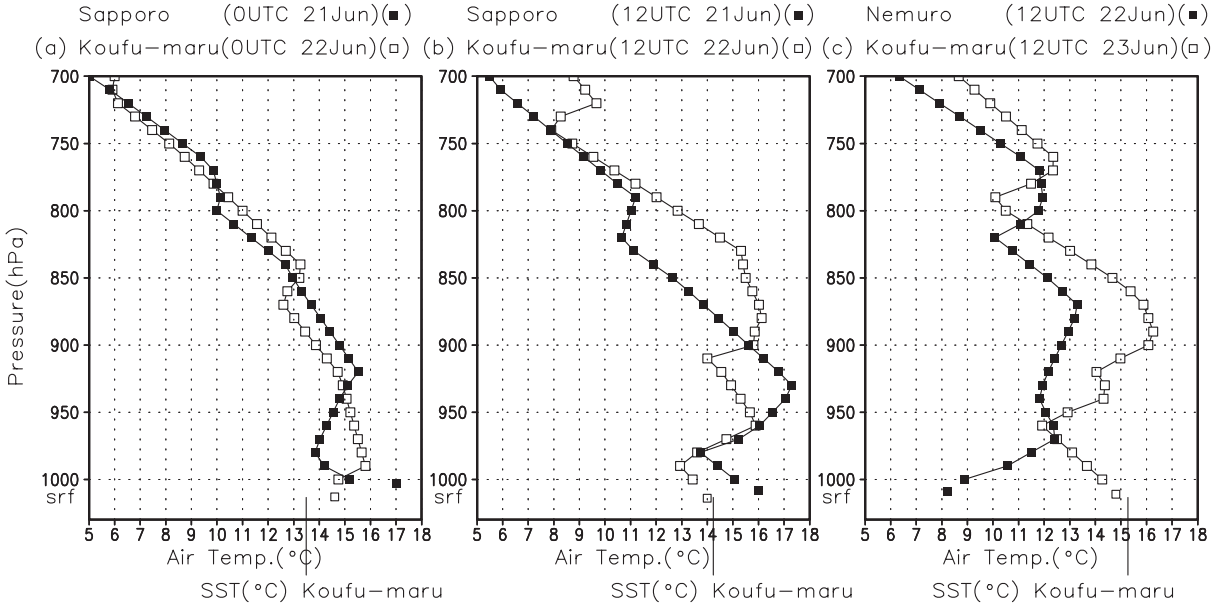

Fig. 5. Profiles of air temperature observed at Sapporo (0 UTC, June 21) and Koufu-maru (0 UTC, June 22) (a), Sapporo (12 UTC, June 21) and Koufu-maru (12 UTC, June 22) (b), and Nemuro (12 UTC, June 22) and Koufu-maru (12 UTC, June 23) (c). The profiles at Sapporo and Nemuro (Koufu-maru) are shown by lines with closed squares (open squares) in 10-hPa intervals. The bottom square of each line indicates the surface pressure and temperature. SST at Koufu-maru is shown at the bottom.

mixed layer increased abruptly. Subsequently, the back trajectory was not from Hokkaido, but from the Okhotsk Sea region (Fig. 4g), where the SST was much lower than in the ocean east of the Sanriku region. Figure 5c shows air temperature profiles at the Koufu-maru site at 12 UTC, June 23, and at Nemuro at 12 UTC, June 22, assuming an approximate 1-day lag between the stations along the back trajectory (Fig. 4h). The temperature profile at Nemuro was employed as a proxy for air on the trajectory from the Okhotsk Sea. The surface air temperature (8.2°C) at Nemuro was much lower than the air temperature (14.8°C) and SST (15.2°C) at the Koufu-maru at 12 UTC, June 23. The large temperature difference and the elongated fetch of the Yamase air indicate that the ocean significantly heated the Yamase air arriving at the Koufu-maru site; this was consistent with the observed well-developed mixed layer at the Koufu-maru site and enlarged cloud droplets (Kojima et al. 2006). Between 6 UTC, June 23, and 6 UTC, June 24, the cloud top height increased continuously (Fig. 2b), and the cloud base increased to 1000 m MSL at 0 UTC, June 24. To examine the changes after 6 UTC, June 23, another analysis method is needed.

Figure 6 shows the time sequence of total (sensible and latent) heat fluxes, along with SST and surface air temperature, along the 2-day back trajectories every 12 h. These were obtained by applying the bulk method (Kondo 1975) to hourly interpolated SST derived from daily NGSST and hourly GPV data for wind, air temperature, and relative humidity at the surface. The symbols A, B, and C on the abscissa in each panel indicate the positions shown in the corresponding panel of Fig. 4. The geographical distribution of the corresponding total heat fluxes every 12 h during the same period are shown in Fig. 7. The figure also shows 4-day averaged SST between 12 UTC, June 20, and 12 UTC, June 24. Three back trajectories of Yamase air on the Koufu-maru at 12 UTC, June 22, 12 UTC, June 23, and 12 UTC, June 24, are shown, along with the locations of the air parcel at the map time of each panel. Note that total heating can be positive despite the SST being lower than the air temperature, when a positive latent heat flux overcasts a negative sensible heat flux (e.g., around B in Fig. 6f).

Before 12 UTC, June 22, heating was weak along the trajectory. Air parcels reached high tempera-

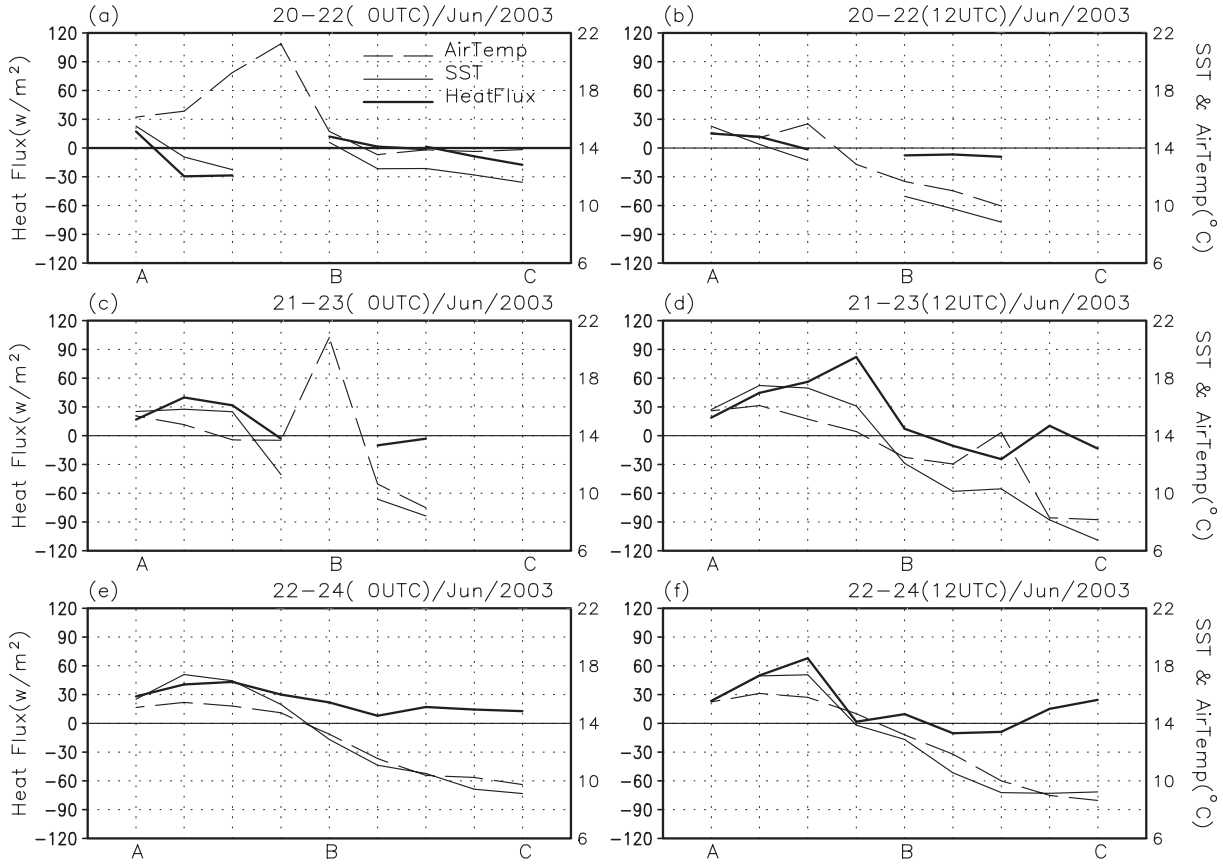

Fig. 6. Time sequence of 6-hourly air temperature (dashed lines), SST (thin solid line), and total heating (thick solid line) along the back trajectories shown in Fig. 4, except every 12 h between 0 UTC, June 22, and 12 UTC, June 24, in 2003. A, B, and C in each panel indicate the time at the same time, 1 day before, and 2 days before, respectively. The SST and total heating for when the air trajectories were over land are not shown.

tures over Hokkaido due to land surface heating. They then experienced negative heating over the sea south off Hokkaido, where the SST was lower than the air temperature (Fig. 6a). After 0 UTC, June 23, air parcels experienced strong heating between Hokkaido and the Sanriku coast, where the SST exceeded the air temperature. The air temperature at B (Fig. 6c) was much higher than those 6 h before and after B. As the temperature at B was interpolated from grid points between warm land (eastern Hokkaido) and cool ocean, air temperature over the ocean near B seemed close to the average of the air temperatures 6 h before and after B. Figure 7f shows that the heating off the Sanriku coast to the west of 144°E was weak. The southward SST gradient was small over the Oyashio intrusion. Strong heating was observed along a subarctic (Oyashio) oceanic front with a large SST gradient around 40°N and between 144°E and 147°E. The back trajectories of Yamase air gradually shifted eastward after 0 UTC, June 23, off the Sanriku coast, crossing the oceanic front after 12 UTC, June 23. The heating along the trajectory thus increased after 12 UTC, June 23. This may have contributed to the upward development of the mixed layer after 0 UTC, June 23 (Fig. 2). The cloud base gradually became lower between 12 UTC and 21 UTC, June 23 (Fig. 2b). This may have been caused by nighttime destabilization due to intensified radiative cooling at the cloud top (Kojima et al. 2006). This process may also have contributed to the upward development of clouds during the period.

Figure 8 shows vertical profiles of the relative hu-

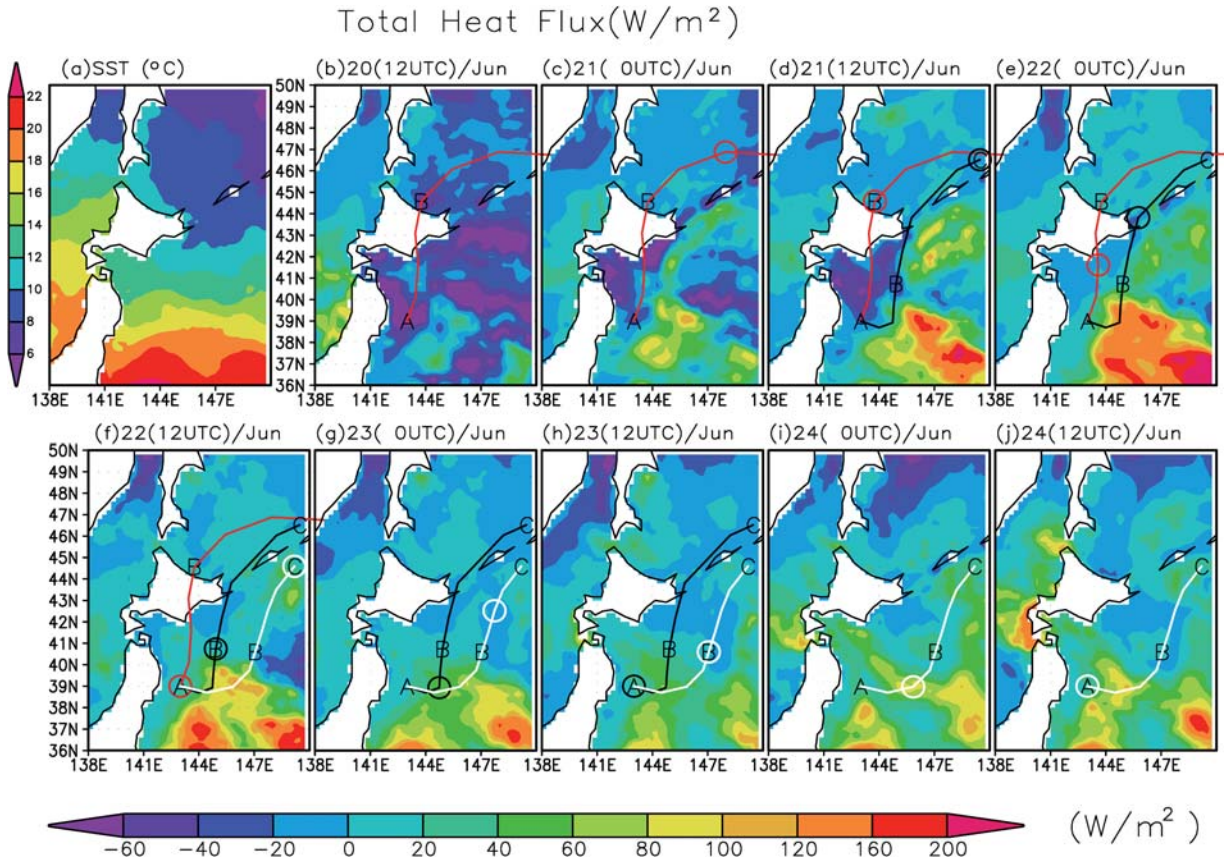

Fig. 7. SST distribution averaged between 12 UTC, June 20, and 12 UTC, June 24, in 2003 (left top panel). Total heat (sensible and latent heat) flux over the ocean every 12 h between 0 UTC, June 20, and 12 UTC, June 24. Back trajectories of air on the Koufu-maru at 12 UTC, June 22 (red lines), at 12 UTC, June 21 (black lines), and at 12 UTC, June 22 (white lines) are also shown. A, B, and C in each panel indicate the air positions at the same time, 1 day before, and 2 days before, respectively. The circles on the trajectory indicate the positions of air parcels for each map time.

midity, temperature, Omega, $Q1/Cp$, $Q2/Cp$, and v-component of 925-hPa wind averaged over the ocean area covered by the four observation sites shown in Fig. 1. The moist layer with relative humidity greater than 90% is shaded in the third and fourth panels as a proxy for cloud layer. We studied $Q1/Cp$ and $Q2/Cp$ in the Yamase cloud layer because these parameters were rather noisy above the clouds. Between 0 UTC, June 22, and 0 UTC, June 23, $Q1/Cp$ and $Q2/Cp$ were almost zero near the bottom layer, below 950 hPa. As convective mixing within shallow clouds developed during this period (Fig. 2), the small $Q1/Cp$ is a result of cancellation between sensible heating over the ocean and radiative cooling at the top of the shallow clouds. In addition, $Q2/Cp$ was small due to partial cancellation of moisture sink within the clouds by the moisture supply from the ocean. Between 0 UTC, June 23, and 12 UTC, June 24, the cloud layer developed upward (Fig. 2). Positive $Q2/Cp$ around 950 hPa between 0 and 12 UTC, June 24, suggested moisture sink by active cloud condensation. Weak negative $Q1/Cp$ appeared near the cloud top after June 23 and increased at 12 UTC, June 23, probably due to radiative cooling. After 12 UTC, June 23, $Q1/Cp$ near the surface became positive and increased until 0 UTC, June 25. This could be ascribed not to heating over the ocean but to land surface heating over Hokkaido, because the southerly landed over Hokkaido in the study region, where the surface air temperature was much higher than that over the water to the south.

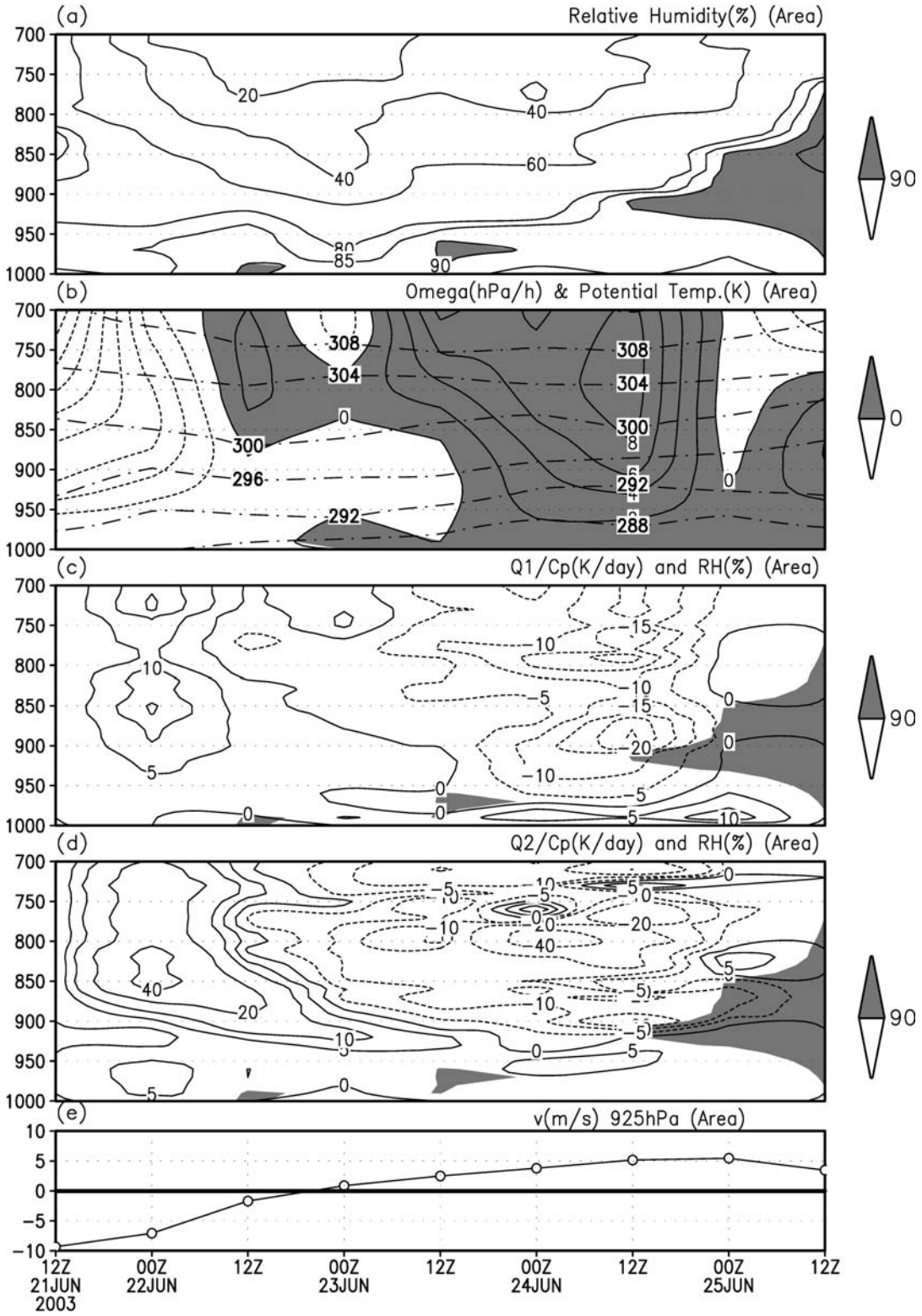

Fig. 8. Profiles of relative humidity (a), vertical p-velocity (Omega) and potential temperature (b), $Q1/Cp$ (apparent heat source) (c), $Q1/Cp$ (apparent heat sink) (d), and the v-component of wind at 925 hPa (e). These values were obtained from profiles at four points (Nemuro, Sapporo, Misawa, and the Koufu-maru).

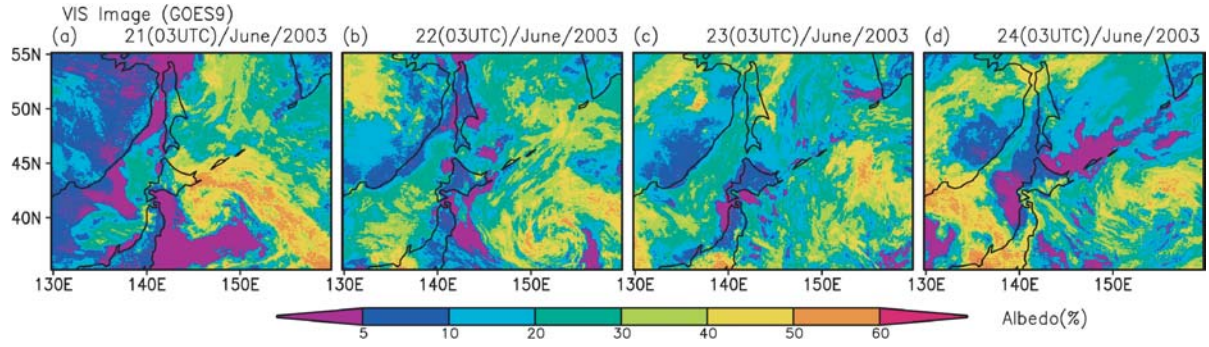

Fig. 9. Daily visible images around northern Japan and the western North Pacific observed by GOES-9 at 3 UTC between June 21 and 24, 2003.

For previous Yamase events, Ninomiya and Mizuno (1985) estimated apparent total heat source of the order of 5 K/day in a Yamase layer over the water off the Sanriku coast. However, in our case, the apparent total heat source $(Q1 - Q2)/Cp$ in the Yamase layer over the water was weaker (2∼4 K/day) between 0 UTC, June 22, and 12 UTC, June 24. In the cases examined by Ninomiya and Mizuno (1985), Yamase clouds with relative humidity greater than 90% extended above the 900 hPa level. The present cloud layer was shallow below the 950 hPa level, and heating at the bottom by the ocean may have offset radiative cooling near the cloud top through vertical mixing within the clouds. The sensible heating $(Q1/Cp)$ by the ocean was weak over the budget study region due to the small air–sea temperature difference (Fig. 3), although Fig. 7 shows the strong positive total heating over the sea east of ∼144°E along 39°N, where the SST gradient was large, especially between 12 UTC June 21 and 12 UTC June 22, and June 24, when cold air blew over the front. However, this area was outside the budget study region.

We now discuss the possible relation between the Omega profiles and the Yamase cloud layer. A subsidence began at 12 UTC, June 22, when the Yamase cloud appeared, and intensified until 12 UTC, June 24, when the Yamase cloud extended upward. This suggested that Yamase clouds developed in the turbulent MBL and were mostly maintained against the subsidence by ocean heating and cloud top radiative cooling. The subsidence may have intensified at a dry layer higher than 850 hPa. After 0 UTC, June 25, the cloud layer extended upward higher than 3000 m MSL (Fig. 2b), and the subsidence weakened. This was most likely caused by the approach of synoptic-scale depression. The wind in the cloud turned westerly in the cloud layer above the 1000 m MSL (Fig. 2). These observations indicated that the cloud layer was not originally Yamase cloud but was maintained by the depression.

Figure 9 shows GOES-9 visible images at 3 UTC on June 21, 22, 23, and 24. We used visible images from approximately 12 LT to describe the distribution of shallow clouds, which are sometimes difficult to observe on infrared images due to the small temperature differences between the sea surface and cloud tops. Hokkaido was almost fair on June 22. Low-level clouds appeared over the sea off the Sanriku district on June 22 and then extended southward and thickened until June 24. This was consistent with the development of Yamase clouds observed on the Koufu-maru (Fig. 2).

Here, we note a relationship between the streak pattern of Yamase clouds observed in satellite images (Fig. 9d) and trajectories of the Yamase flow. At 3 UTC, June 24, streaked Yamase clouds covered the water to the south of Hokkaido and the southern part of Hokkaido. These streaks of cloud extended from the northwest to the southeast. Figure 10 shows the corresponding SLP field averaged between 0 and 6 UTC, June 24. This direction of cloud streaks was quasi-parallel to the contours of SLP and quite different from the back trajectories of Yamase air at both 0 and 6 UTC, June 24. The low-level air traveled westward in the last 3 days (Fig. 4). The cloud streaks extended along the wind direction (SSE), whereas the profiles of Yamase clouds were more strongly related to the history of Yamase air along trajectories over the ocean.

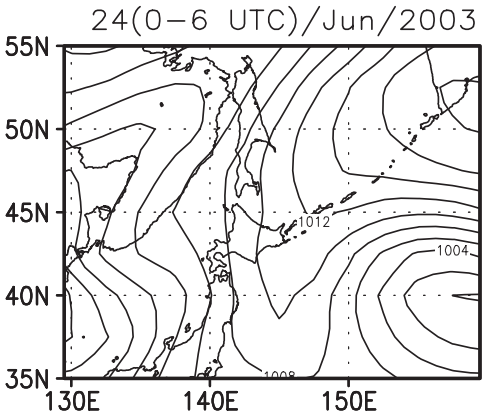

Fig. 10. Sea-level pressure averaged between 0 and 6 UTC, June 24, in 2003.

4. July 2006 event

In early July 2006, an Okhotsk High stagnated over the Okhotsk region, and Yamase flow was observed at the Koufu-maru site around 38.5°N and 142.5°E, east of the Sanriku district. Figure 11 shows the vertical structure of potential temperature and relative humidity at the site. The areas with relative humidity greater than 90% are shaded as a proxy for the cloud layer. The time variations of surface air temperature, SST, visibility, and temperature minus dew point (moist number) observed from the Koufu-maru site are also shown in Fig. 11. Before 0 UTC, July 8, a shallow stable and moist layer was attached to the sea surface, whereas after 0 UTC, July 8, the moist layer detached from the sea surface and extended upward, with decreased stability near the surface. The vertical profiles in the former and latter cases, respectively, were similar to those of the stable layer and mixed layer types proposed by Kodama (1997). The surface moist number also indicated that the surface air was wetter in the former period. The visibility decreased almost to zero at around 18 to 0 UTC in the former period but was continuously high in the latter period. These changes were consistent with the features of each type proposed by Kodama (1997), i.e., surface air is wet and sea fog may appear in the stable layer type, and surface air is unsaturated and low-level clouds are detached in the mixed layer type. Kodama (1997) also noted that the surface air temperature is higher (lower) than the SST in the stable layer (mixed layer) type. However, no such relation between the SST and surface air temperature was clearly observed in the two periods in Fig. 11.

We then examined the back trajectory for each period. Figure 12 shows the 3-day averaged SLP and back trajectories from the 120–160 m MSL at the Koufu-maru site. The corresponding time sequences of total heating, SST, and air temperature along the trajectories are shown in Fig. 13. On July 4, the Okhotsk High appeared, but the low-level airflow at the site was from the south (Fig. 12a). The airflow was thus not the Yamase. As it was cooled by a relatively colder ocean, a shallow stable layer with low-level clouds attached to the surface was observed. After July 5, the trajectory turned westward and continued in this direction until July 8 (Figs. 12b–e). During this period, warm advection was expected, because the SST gradient was large in the upstream of the Koufu-maru site over an oceanic front extending in the WSW–ENE direction around 144°E–146°E (Fig. 1). The SST was lower than the surface air temperature between A and B in Fig. 13c. Between 0 and 12 UTC, July 8, the trajectory began to meander (Figs. 12e, f). After 0 UTC, July 9, the southward Yamase airflow shifted east and crossed an oceanic front (to the east of 145°E along 40.5°N) with a large SST gradient. The total positive heating increased at this time (Fig. 13). This heating may have contributed to the disappearance of the atmospheric stable layer near the surface and to the development of the atmospheric mixed layer after July 9 shown in Fig. 11. On July 10, trajectories turned northwestward near the Koufu-maru. However, the surface stable layer was not recovered (Fig. 11). This may have been because the short fetch was not sufficient to form a stable layer, because Yamase air passed over an oceanic front crossing a sharp angle different from the case for July 5–8. It may take a longer fetch to develop stable layer type stratification by bottom cooling than to develop mixed layer type stratification by bottom heating.

Kodama (1997) noted that the local surface air temperature minus the SST was positive (negative) for stable layer (mixed layer) type stratification in the Yamase in the summer of 1993, as observed at Misawa. However, for the present case, no such relation was clearly observed, e.g., the surface air temperature was higher than the SST at the Koufu-maru site after 12 UTC, July 8 (Fig. 11), although the mixed layer type stratification was observed for the period. The SST of water off Misawa decreased gradually to the north (Fig. 1). It can

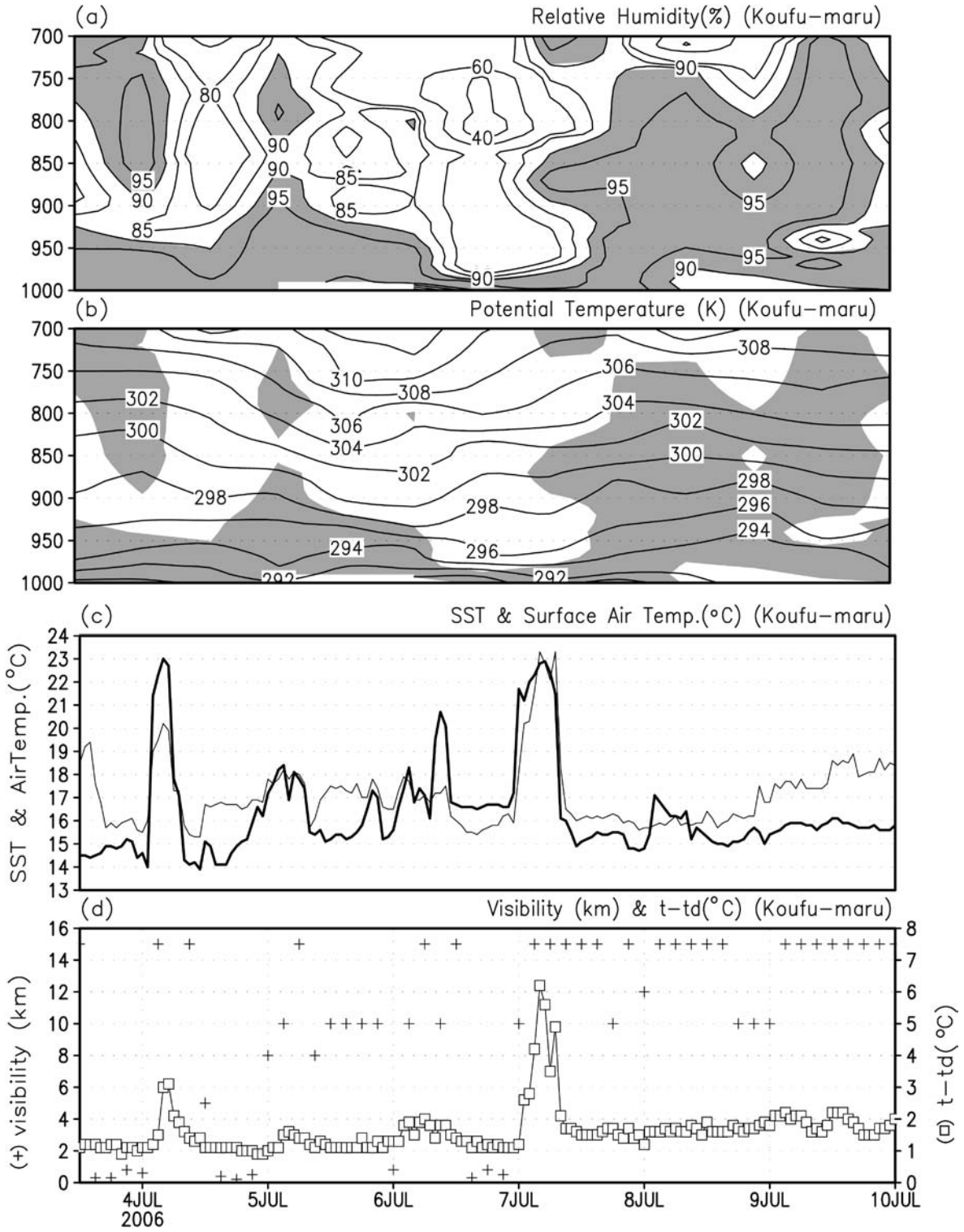

Fig. 11. Profiles of relative humidity (%) (a) and potential temperature (K) (b) at the Koufu-maru site around 38.5°N and 142.5°E between 0 UTC, July 4, and 0 UTC, July 10, in 2006. Relative humidities of $> 95\%$ are shaded in both panels, along with the SST (thick line) and surface air temperature (thin line) (c), and visibility (cross) and moist number (temperature minus dew point; open square) (d).

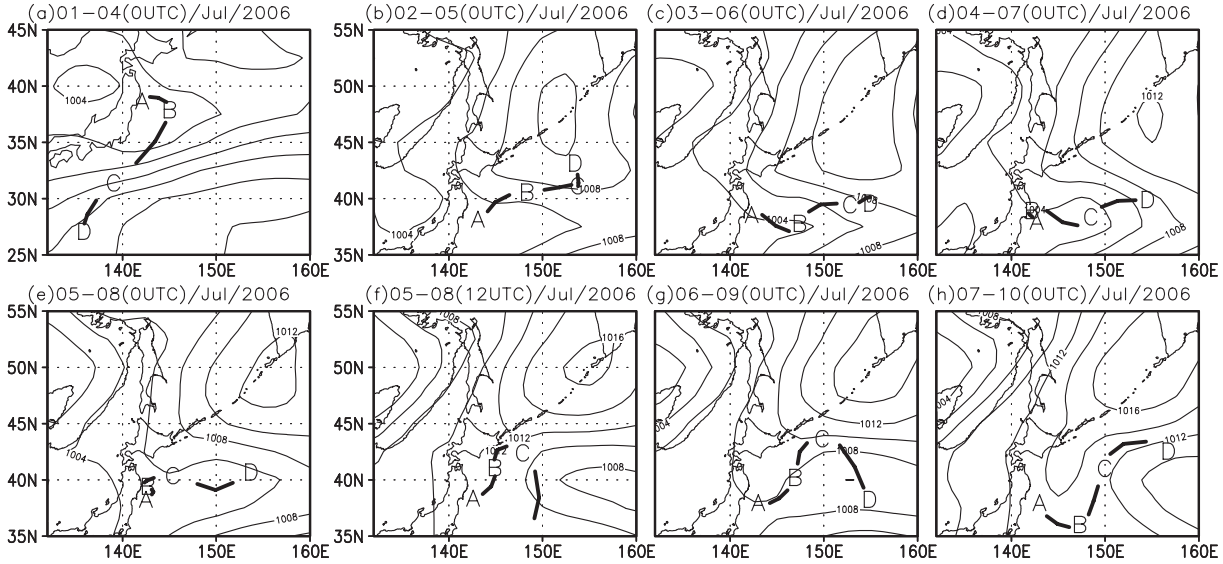

Fig. 12. As in Fig. 4, except for low-level air at 120 m MSL (160 m MSL for the trajectories for July 9 and 10) at the Koufu-maru site around 38.5°N and 142.5°E between 0 UTC, July 4, and 0 UTC, July 16, in 2006.

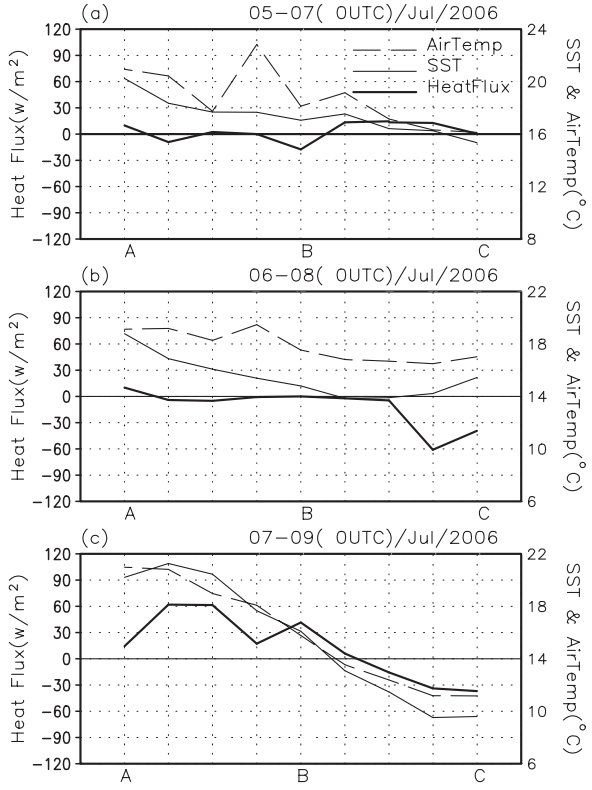

Fig. 13. As in Fig. 6, except daily between 0 UTC, July 7 and July 9, in 2006.

take a long fetch to form a stable layer type under the conditions of warm advection. The Koufu-maru site was close to or within an oceanic front at the southern edge of the Oyashio intrusion. The distance from the oceanic front to the east of 144°E was also short. Therefore, it is difficult to take a sufficient fetch to form a stable layer type stratification near the Koufu-maru site. After the development of mixed layer type stratification over the oceanic front, recovering stable layer type stratification by bottom cooling was difficult by warm advection. For example, in the case of July 10 (Fig. 12h), the trajectory turned northwestward near the Koufu-maru site, but stable layer type stratification was not significant (Fig. 11b).

Figure 14 shows the time variations of vertical profiles of Omega and the results of heat budget analysis as shown in Fig. 8. There was a relationship between Omega and the vertical structure of the Yamase cloud layer. Strong subsidence dominated between 0 UTC, July 4, and 0 UTC, July 7 (Fig. 14b). This may have confined the cloud layer below the 920–950 hPa level (Fig. 14a). Strong negative $Q1/Cp$ (cooling) and $Q2/Cp$ (moistening) were observed near the top of the moist layer, especially at 0 UTC, July 6 (Figs. 14c, 14d). Radiative cooling and evaporation of cloud droplets, which were suggested by moistening at the cloud top, may have caused cooling. The moist layer above

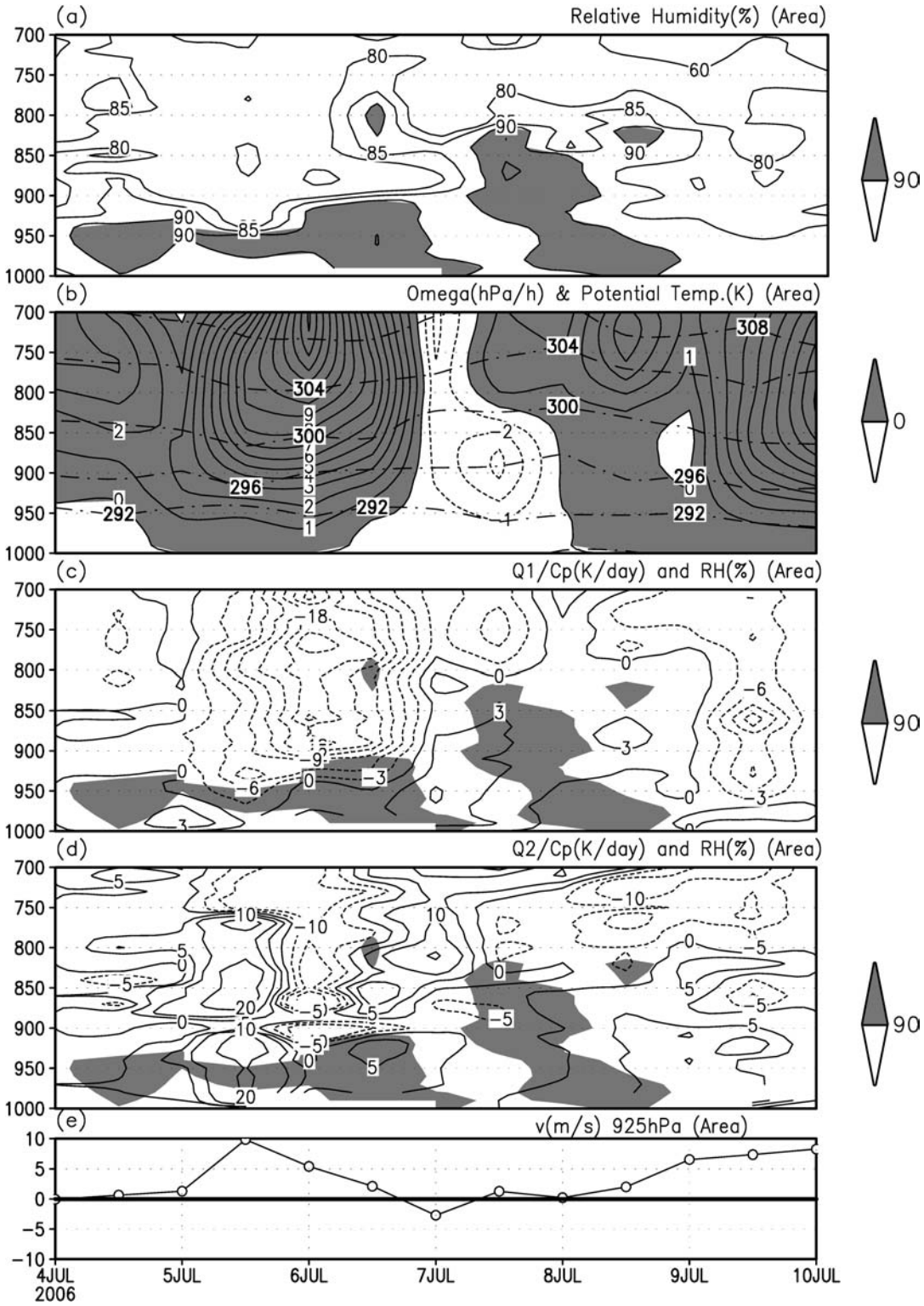

Fig. 14. As in Fig. 8, except between 0 UTC, July 4, and 0 UTC, July 10, in 2006.

the ocean surface was characterized by weak heating (positive $Q1/Cp$) and drying (positive $Q2/Cp$). This suggested condensation heating in the clouds, although $Q2/Cp$ between 0 UTC, July 5, and 0 UTC, July 7, was noisy. Between 0 UTC, July 7, and 0 UTC, July 8, the subsidence disappeared, and a weak updraft appeared. In this period, stability was weakened in the lower layer, and the moist layer extended up to 800 hPa (Figs. 11a, b). Positive $Q1/Cp$ and $Q2/Cp$ were observed in the moist layer above 950 hPa (Figs. 14c, d). These observations suggested that diabatic heating by condensation occurred. After 0 UTC, July 8, subsidence recovered and cloud layer became shallower. Cloud layer disappeared after 0 UTC, July 9, when subsidence was intensified. In the June 2003 case, the stepwise development of Yamase cloud layer was explained by the history of heating and cooling on the trajectories, whereas in the July 2006 case, the development of the Yamase cloud layer was influenced by both history and vertical wind.

During the study period, no apparent strong total heating $(Q1 - Q2)/Cp$ due to oceanic heating was found near the surface, except at 12 UTC, July 5, when a large $Q2/Cp$ appeared[2] between the surface and 750 hPa level. As shown in Fig. 13 and as noted previously by Tomiya and Asano (2008), strong heating occurred over the sea southeast of the ship site when cold advection occurred. The budget analysis region used in the present study was outside the region of strong heating by the ocean.

5. Conclusions

Despite the strong influence of air–sea interaction on the Yamase and associated boundary layer clouds, there have been few in situ observations of the Yamase over the ocean. Campaign observations of the Yamase were performed for 7 summers from 2001 to 2007 inclusive, and invaluable aerological data over the ocean were obtained by the JMA vessel Koufu-maru. We examined the vertical structure of the maritime atmosphere and clouds, and air mass transformation processes along Yamase airflow trajectories for two Yamase events using the campaign observation data.

The case study for the June 2003 dealt with the initial stage of a long-lasting Yamase event. The direction of Yamase flow toward the vessel was south or southwestward throughout the study period but gradually shifted eastward. Vertical development of Yamase clouds was observed according to the change of trajectories influenced by land and an oceanic front. Three stages were found in stepwise development of Yamase clouds (Kojima et al. 2006). In the first stage, when a thin and low cloud layer (top at 300 m MSL) appeared over the Koufu-maru site, the low-level airflow was from the north crossing over Hokkaido, where the air was relatively dry and warm. When the northerly began from Hokkaido, a shallow stable layer appeared due to cooling by the sea. Then shallow Yamase clouds appeared, and a shallow mixed layer developed in a thin cloud layer. In the second stage, the cloud top developed upward and the cloud base rose, detaching from the sea surface. A convective mixed layer accompanying low-level clouds was observed. In this period, the Yamase air at the Koufu-maru site was from the Okhotsk Sea, passing over the ocean east of Hokkaido. This was a cold advection, which may have enhanced convection in the mixed layer by heating from the sea. In the third stage, the cloud top increased and the cloud base jumped to 1000 m MSL. This change was ascribed to the eastward shift of the trajectories of Yamase air, which passed over an oceanic front with a large SST gradient, where strong heating may occur in cold advection.

In the case study for the July 2006 Yamase event, Yamase flow over the ocean changed between westward and southward, in contrast to the case of June 2003 when Yamase flow was southwestward. According to the change in wind direction, the vertical structures of MBL at the Koufu-maru site changed between stable layer type when westward and mixed layer type when southwestward. Visibility at the surface decreased during the stable layer type. These two structure types were similar to those proposed by Kodama (1997). Back trajectory analysis indicated that the observed alternation was related to the increase in heat flux over the ocean due to the intensified cold advection of Yamase air. In the study reported by Kodama (1997), local air–sea temperature differences were related to the structure type of Yamase MBL. In our case, no such clear correspondence was observed. History of

2 Strong $Q2/Cp$ variation was also found on July 6 above the 920 hPa level, but corresponding variation was not significant in $Q1/Cp$. During the period, relative humidity changed significantly only at Misawa and the Koufu-maru site. Partial moistening and drying within the budget study area caused these variations in $Q2/Cp$. Moistening by seeding from upper clouds is a possible reason for the change in humidity.

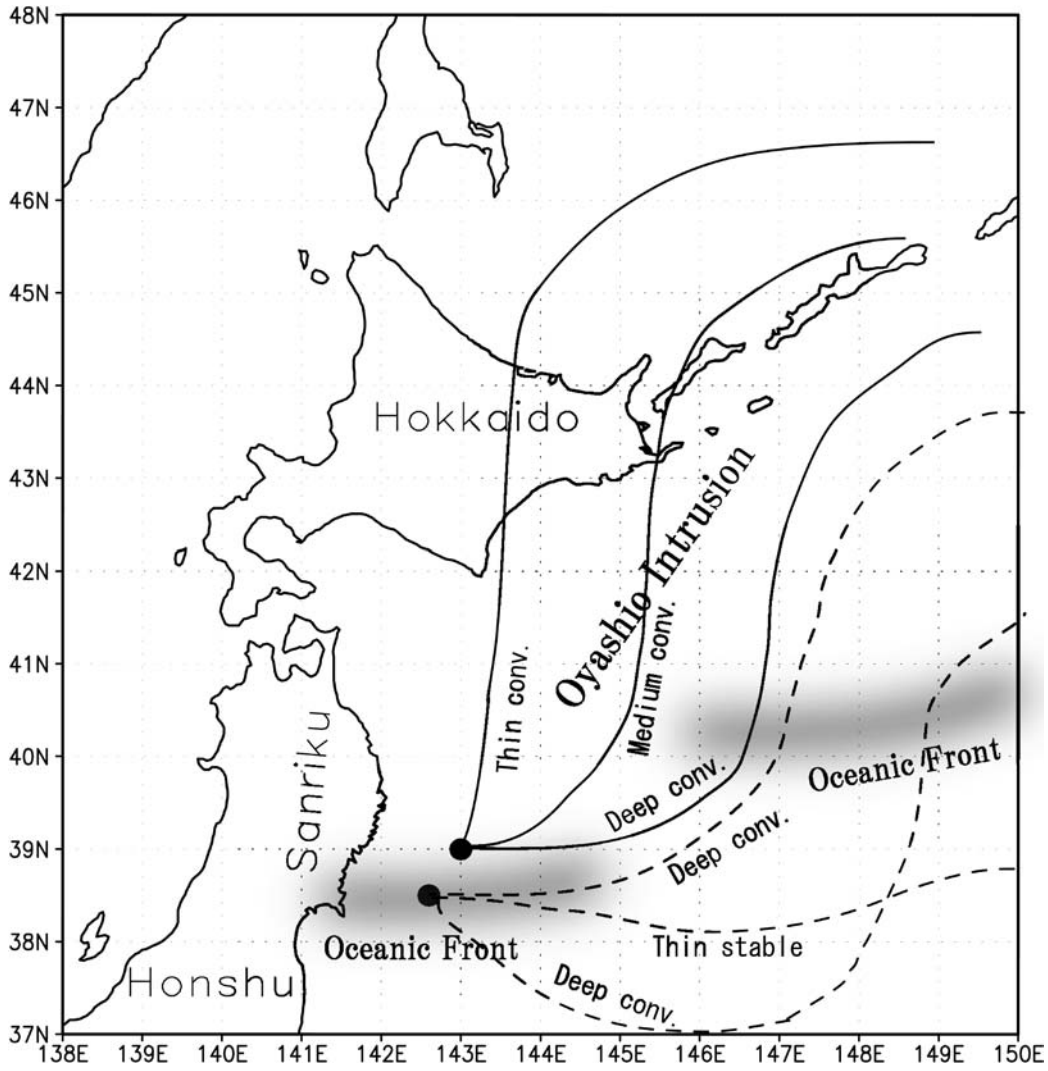

Fig. 15. Conceptual model of stratification of Yamase cloud layer observed at the Koufu-maru site related to back representative trajectories examined in this study. Solid lines are the trajectories in June 2003 cases and dashed lines are in July 2006 cases.

modification of air in upstream area, especially over oceanic fronts, was more important for determining the structure of MBL in our case. This was because the Koufu-maru site was close to oceanic fronts where strong heating by the ocean occurred, whereas Misawa, which is where Kodama's (1997) study was performed, was far from the oceanic fronts, and low-level stratification was determined according to local sea surface flux on the fetch after leaving the oceanic fronts. Figure 15 shows a schematic representation of the relationship between stratification of the Yamase cloud layer observed at the Koufu-maru site and several back trajectories examined in this study. Solid lines are representative trajectories in June 2003 cases and dashed lines are in July 2006 cases.

We performed heat and moisture budget analyses for the Yamase flow over the sea near the Sanriku coast, which was surrounded by four observation sites, including the Koufu-maru. The stratification of the lower troposphere was influenced by back trajectories of the Yamase and by vertical wind. The Yamase clouds were accompanied by moisture sink, which suggested latent heating. However, sen-

sible heating was not large in the clouds, probably due to weak heating over the ocean with a small air–sea temperature difference and to strong radiative cooling at the top of the clouds. The prediction of weak heating over coastal water is consistent with previous studies (e.g., Ninomiya and Mizuno 1985). Our budget study region was far from the oceanic fronts east of 144°E, along which strong heating may occur.

Recently, the influence of oceanic fronts in the mid-latitudes on the MBL has been described as ocean-to-atmosphere feedback. Nonaka and Xie (2003) studied the correlations over the Kuroshio extension south of our study area using satellite observations. They pointed out that the surface wind is stronger (weaker) over warm (cold) SST anomalies. Spall (2007) examined the modification of atmospheric MBL over oceanic fronts using numerical experiments. Oceanic fronts, which may affect Yamase air, were observed east of 144°E and north of 40°N in the Oyashio extension (Nonaka et al. 2006). The upward development of Yamase clouds over the oceanic fronts seems to be a significant example of ocean-to-atmosphere feedback. There have been relatively few *in situ* observations of air–sea interaction over mid-latitude oceanic fronts. Further studies of air–sea interaction around the oceanic fronts of the Oyashio extension are required to examine the transformation of the Yamase air mass. The influence of Yamase flow to the ocean is another important area for future study. It may be significant, because cool and wet Yamase may decrease SST by long-lasting reduction of sunshine and upward sensible heat flux.

Acknowledgments

This study was supported by the Ministry of Education, Culture, Sports, Science and Technology (MEXT) of Japan under two Grants-in-Aid for Scientific Research supervised by Prof. S. Asano of the CAOS, Tohoku University (17204039), and by Prof. T. Tsuda of the Research Institute of Sustainable Humanosphere (RISH), Kyoto University (19403009). We thank the HMO, JMA, for providing the aerological data collected on the Koufu-maru. The trajectory analysis system used was developed by CGER-METEX. The New Generation Sea Surface Temperature (NGSST) data were provided by the NGSST development group, which is directed by Prof. H. Kawamura of Tohoku University. The Grid Point Value data were provided by JMA and distributed by RISH of Kyoto University.

References

Gorai, M., and H. Sasaki, 1990: Process of intrusion and modification of Yamase (in Japanese). *Kaiyo Monthly*, **22**, 386–390.

Guan, L., and H. Kawamura, 2004: Merging satellite infrared and microwave SSTs: Methodology and evaluation of the new SST. *J. Oceanogr.*, **60**, 905–912.

Kodama, Y.-M., 1997: Airmass transformation of the Yamase airflow in the summer of 1993. *J. Meteor. Soc. Japan*, **75**, 737–751.

Kojima, M., S. Asano, and H. Iwabuchi, 2006: Time-variations of optical and microphysical properties of Yamase clouds estimated from shipboard experiments and satellite remote sensing in June 2003. *SOLA*, 045–048, doi:10.2151/sola.2006-012.

Kondo, J., 1975: Air-sea bulk transfer coefficients in diabatic conditions. *Boundary-Layer Meteorol.*, **9**, 91–112.

Nagasawa, R., T. Iwasaki, S. Asano, K. Saito, and H. Okamoto, 2006: Resolution dependence of non-hydrostatic models in simulating the formation and evolution of low-level clouds during ''Yamase'' event. *J. Meteor. Soc. Japan*, **84**, 969–987.

Ninomiya, K., and H. Mizuno, 1985: Anomalously cold spell in summer over northeastern Japan caused by northeasterly wind from polar maritime airmass Part 2. Structure of the northeasterly flow from polar maritime airmass. *J. Meteor. Soc. Japan*, **63**, 859–871.

Nonaka, M., H. Nakamura, Y. Tanimoto, T. Kagimoto, and H. Sasaki, 2006: Decadal variability in the Kuroshio–Oyashio extension simulated in an eddy—resolving OGCM. *J. Climate*, **19**, 1970–1989.

Nonaka, M., and S.-P. Xie, 2003: Covariations of sea surface temperature and wind over the Kuroshio and its extension: evidence for ocean-to-atmosphere feedback. *J. Climate*, **16**, 1404–1413.

O'Brien, J. J., 1970: Alternative solutions to the classical vertical velocity problem. *J. Appl. Meteor.*, **9**, 197–203.

Spall, M. A., 2007: Mid-latitude wind stress—sea surface temperature coupling in the vicinity of the oceanic front. *J. Climate*, **20**, 3785–3801.

Takai, H., H. Kawamura, and O. Isoguchi, 2006: Characteristics of the Yamase winds over oceans around Japan observed by the scatterometer-derived ocean surface vector wind. *J. Meteor. Soc. Japan*, **84**, 365–373.

Tomiya, Y., and S. Asano, 2008: A study of air-sea interactions during Yamase events from shipboard experiments over the eastern waters off the Sanriku coast (in Japanese). *Kaiyo Monthly*, special issue **49**, 27–33.

Urano, A., K. Nakamura, and T. Asai, 1990: Formation of low-level clouds over ocean and influence of ra-

diation cooling during Yamase periods (in Japanese). *Kaiyo Monthly*, **22**, 411–416.

Yanai, M., S. Esbensen, and J.-H. Chu, 1973: Determination of bulk properties of tropical cloud clusters from large-scale heat and moisture budgets. *J. Atmos. Sci.*, **30**, 611–627.

Yanai, M., and R. H. Johnson, 1993: Impacts of cumulus convection on thermodynamic fields. The representation of cumulus convection in numerical models of the atmosphere. *Meteor. Monogr.*, **46**, *Amer. Meteor. Soc.*, 39–62.

Yanai, M., C. Li, and Z. Song, 1992: Seasonal heating of the Tibetan Plateau and its effects on the evolution of the Asian summer Monsoon. *J. Meteor. Soc. Japan*, **70**, 319–351.

Yuan, X., and L. D. Talley, 1996: The subarctic frontal zone in the North Pacific: Characteristics of frontal structure from climatological data and synoptic surveys. *J. Geophys. Res.*, **101**, 16491–16508.

Zeng, J., M. Katsumoto, R. Ide, M. Inagaki, H. Mukai, and Y. Fujinuma, 2003: Development of meteorological data explorer for Windows. Data Analysis and Graphic Display System for Atmospheric Research using PC, ed. by Y. Fujinuma, CGER-M014-2003, *Center for Global Environmental Research*, NIES, 19–73.